Available online at www.sciencedirect.com
SCIENCE DIRECT®
Journal of Magnetic Resonance 171 (2004) 345–352
JMR Journal of Magnetic Resonance
www.elsevier.com/locate/jmr

Analysis of longitudinal multispin orders in strongly coupled spin systems

S. Sendhil Velan*

Center for Advanced Imaging and Radiology, West Virginia University, Morgantown, WV 26506, United States

Received 29 July 2004; revised 30 August 2004
Available online 13 October 2004

Abstract

Longitudinal multispin orders provide an effective way for measurement of scalar couplings and also to probe molecular interactions and dynamics. Analysis of longitudinal orders has been made in strongly coupled AB and ABX spin systems to determine the dependence of strong coupling parameter on these orders. Experimental and simulated spectra of various longitudinal orders are illustrated for these spin systems. This general procedure can be extended to broad range of spin systems to understand the influence of strong coupling on longitudinal orders.

Keywords: Longitudinal multispin orders; Strong coupling; Zero quantum coherence; Frequency cycling; Spectral editing

1. Introduction

Longitudinal multispin orders correspond to the non-equilibrium population distribution and can be created in spin systems that exhibit J couplings, dipolar couplings or quadrupolar couplings [1,2]. They provide information on molecular connectivity, geometry, and dynamics [1]. The longitudinal orders are also referred as magnetization modes which are used to analyze the longitudinal relaxation in coupled spin systems [3–5]. In solution state, longitudinal multispin orders can be created in molecules that exhibit scalar couplings. Longitudinal orders serve as an intermediate state in many polarization transfer experiments [6–11] and sequences using multispin orders have been designed for editing different metabolites like lactate and GABA [9–11]. Three-spin longitudinal orders (homonuclear) have been created by a polarization transfer sequence employing non-selective pulses [6] or transition selective frequency cycling approach [12] that utilize shaped RF pulses for determination of relative sign of coupling constants. Sequences employing non-selective pulses edit even and odd longitudinal orders by a π pulse. It is possible to achieve editing of various longitudinal orders in analogy to distortionless enhancement by polarization transfer (DEPT) editing sequence [13] by varying the reconversion flip angle that converts longitudinal order into observable magnetization and performing suitable weighted linear combination of the resulting signal.

The spin systems can be classified as weakly and strongly coupled depending on the magnetic field strength that is employed. The distinction between the two is the relative magnitude of scalar coupling constant J between two spins and the difference of their Larmor frequencies [1,2]. Longitudinal orders have been investigated in weakly coupled spin systems where the chemical shift part of the Hamiltonian is larger than the J coupling part of the Hamiltonian [12]. Our goal was to investigate the effect of strong coupling parameter on various longitudinal orders. Exact results are obtained showing the dependence of the strong coupling on

* Fax: +1 304 293 4287.
E-mail address: svelan@hsc.wvu.edu.

1090-7807/$ - see front matter © 2004 Elsevier Inc. All rights reserved.
doi:10.1016/j.jmr.2004.09.012

various longitudinal orders in a strongly coupled two-spin 1/2 (AB) and three-spin 1/2 (ABX) systems. This approach can easily be extended to other strongly coupled systems. At lower magnetic field strengths like 1.5 and 3 T (routinely used for clinical applications) most of the molecules observed in various pathologies exhibit strong coupling. The solutions provided here will be of significance for spectral editing sequences using longitudinal orders and also for two-dimensional techniques that involve multispin order pathways.

2. Theory

The isotropic Hamiltonian of a spin system in solution state will consist of a Zeeman part describing the magnetic interaction of nuclear spins with the static field and the indirect J coupling describing the interaction of pairs of nuclear spins through bonding electron given by

$$H = \sum_i \omega_i I_{iz} + \sum_{i,j(i<j)} 2\pi J_{ij}(I_{iz}I_{jz} + I_{ix}I_{jx} + I_{iy} + I_{jy}). \quad (1)$$

When $2\pi J_{ij} \ll |\omega_i - \omega_j|$, the system is said to be weakly coupled, and the Hamiltonian can be approximated by

$$H = \sum_i \omega_i I_{iz} + \sum_{i,j(i<j)} 2\pi J_{ij} I_{iz} I_{jz}. \quad (2)$$

Here, I_m $(m = x, y, z)$ refers to the components of the nuclear spin angular momentum operators, ω_i refers to the precession frequency of the nuclei, and J_{ij} is the scalar coupling constant between spins i and j. The values of J_{ij} depend on the covalent bonds connecting spins i and j. They normally have a small range (<50 Hz) and become very small (<1 Hz) if the spins are connected by more than 4–5 bonds. When the chemical shift difference of two-coupled spins becomes comparable to that of the scalar couplings, the Zeeman and the coupling parts of the Hamiltonian do not commute. Therefore, the eigenstates of strongly coupled spins are obtained as the linear combination of the product states of various spins. The eigenstates for various strongly coupled spin systems have been previously solved [14,15]. Various theoretical approaches have been employed for describing strongly coupled spin systems [1,16,17]. In this study, the transition selective approach is employed for obtaining solutions to determine the response of any arbitrary flip angle on each transition of strongly coupled AB and ABX spin systems.

2.1. AB spin system

In an AB spin system, the chemical shift difference $(\omega_A - \omega_B)$ is comparable with the magnitude of the coupling constant J_{AB} between the A and B spins. The Hamiltonian for strongly coupled AB (spin 1/2) system can be expressed as

$$H = \omega_1 I_{1z} + \omega_2 I_{2z} + 2\pi J_{12}(I_{1z}I_{2z} + I_{1x}I_{2x} + I_{1y}I_{2y}). \quad (3)$$

I_{1m} and I_{2m} are the m-components of the nuclear spin angular momentum operators for A and B nuclei; ω_1 and ω_2 are the precession frequencies of A and B nuclei and J_{12} is the scalar coupling constant. A number of biologically important molecules exhibit AB spectral characteristics. For example, citrate (which is an important metabolite marker for prostate cancer [18]) is an AB spin system. The eigenstates for the AB spin system are $|\alpha\alpha\rangle$, $\cos\theta|\alpha\beta\rangle + \sin\theta|\beta\alpha\rangle$, $\cos\theta|\beta\alpha\rangle - \sin\theta|\alpha\beta\rangle$, and $|\beta\beta\rangle$ where $\theta = \frac{1}{2}\tan^{-1}(\frac{2\pi J_{AB}}{\omega_A - \omega_B})$ is the mixing angle. In weak coupling limit, the angle θ is very small and the eigenstates will be $|\alpha\alpha\rangle$, $|\alpha\beta\rangle$, $|\beta\alpha\rangle$, and $|\beta\beta\rangle$ for the two-spin 1/2 system [1,2]. The energy level diagram with the eigenstates of the AB spin system is shown in Fig. 1.

The transition selective Hamiltonian for each of the four AB transitions can be expressed in terms of shift and polarization operators. The solutions for the effect of x phase transition selective pulse with arbitrary flip angle β on the equilibrium density matrix $\rho_0 = I_{1z} + I_{2z}$ is given for the four transitions:

$$\begin{aligned}|1\rangle\langle 2| \Rightarrow\ & I_{1z}\left(\tfrac{1}{2}\sin^2\theta(\cos\beta - 1) + 1\right) + I_{1z}I_{2z}(\cos\beta - 1)\\ & + I_{2z}\left(\tfrac{1}{2}\cos^2\theta(\cos\beta - 1) + 1\right) - I_{1z}I_{2y}\cos\theta\sin\beta\\ & - I_{1y}\tfrac{1}{2}\sin\theta\sin\beta - I_{2y}\tfrac{1}{2}\cos\theta\sin\beta\\ & - (I_{1y}I_{2y} + I_{1x}I_{2x})\cos\theta\cdot\sin\theta(\cos\beta - 1)\\ & - I_{1y}I_{2z}\sin\theta\sin\beta, \end{aligned} \quad (4)$$

$$\begin{aligned}|3\rangle\langle 4| \Rightarrow\ & I_{1z}\left(\tfrac{1}{2}\sin^2\theta(\cos\beta - 1) + 1\right) - I_{1z}I_{2z}(\cos\beta - 1)\\ & + I_{2z}\left(\tfrac{1}{2}\cos^2\theta(\cos\beta - 1) + 1\right) + I_{1z}I_{2y}\cos\theta\sin\beta\\ & + \tfrac{1}{2}I_{1y}\sin\theta\sin\beta - \tfrac{1}{2}I_{2y}\cos\theta\sin\beta\\ & - (I_{1y}I_{2y} + I_{1x}I_{2x})\cos\theta\cdot\sin\theta(\cos\beta - 1)\\ & - I_{1y}I_{2z}\sin\theta\sin\beta, \end{aligned} \quad (5)$$

$$\begin{aligned}|3\rangle\langle 1| \Rightarrow\ & I_{1z}\left(\tfrac{1}{2}\cos^2\theta(\cos\beta - 1) + 1\right) + I_{1z}I_{2z}(\cos\beta - 1)\\ & + I_{2z}\left(\tfrac{1}{2}\sin^2\theta(\cos\beta - 1) + 1\right) + I_{1z}I_{2y}\sin\theta\sin\beta\\ & - I_{1y}\tfrac{1}{2}\cos\theta\sin\beta + I_{2y}\tfrac{1}{2}\sin\theta\sin\beta\\ & + (I_{1y}I_{2y} + I_{1x}I_{2x})\cos\theta\cdot\sin\theta(\cos\beta - 1)\\ & - I_{1y}I_{2z}\cos\theta\sin\beta, \end{aligned} \quad (6)$$

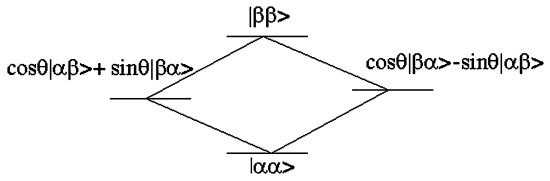

Fig. 1. Energy level diagram of an AB spin system consisting of two-spin 1/2 nuclei.

Table 1
Longitudinal orders and ZQCs created in the four transitions in AB spin system by a x phase transition selective pulse with a flip angle $\beta = 180°$

	$\|1\rangle\langle 2\|$	$\|3\rangle\langle 4\|$	$\|1\rangle\langle 3\|$	$\|2\rangle\langle 4\|$
One-spin order	$-I_{1z}\sin^2\theta + I_{1z}$	$-I_{1z}\sin^2\theta + I_{1z}$	$-I_{1z}\cos^2\theta + I_{1z}$	$-I_{1z}\cos^2\theta + I_{1z}$
	$-I_{2z}\sin^2\theta + I_{2z}$	$-I_{2z}\sin^2\theta + I_{2z}$	$-I_{2z}\cos^2\theta + I_{2z}$	$-I_{2z}\cos^2\theta + I_{2z}$
Two-spin order	$-2I_{1z}I_{2z}$	$2I_{1z}I_{2z}$	$-2I_{1z}I_{2z}$	$2I_{1z}I_{2z}$
	$2(I_{1x}I_{2x} + I_{1y}I_{2y})$	$2(I_{1x}I_{2x} + I_{1y}I_{2y})$	$-2(I_{1x}I_{2x} + I_{1y}I_{2y})$	$-2(I_{1x}I_{2x} + I_{1y}I_{2y})$
ZQC	$\sin\theta \times \cos\theta$	$\sin\theta \times \cos\theta$	$\sin\theta \times \cos\theta$	$\sin\theta \times \cos\theta$

$$
\begin{aligned}
|4\rangle\langle 2| \Rightarrow\ & I_{1z}\left(\tfrac{1}{2}\cos^2\theta(\cos\beta - 1) + 1\right) - I_{1z}I_{2z}(\cos\beta - 1) \\
& + I_{2z}\left(\tfrac{1}{2}\sin^2\theta(\cos\beta - 1) + 1\right) + I_{1z}I_{2y}\sin\theta\sin\beta \\
& - \tfrac{1}{2}I_{1y}\cos\theta\sin\beta - \tfrac{1}{2}I_{2y}\sin\theta\sin\beta \\
& + (I_{1y}I_{2y} + I_{1x}I_{2x})\cos\theta\cdot\sin\theta(\cos\beta - 1) \\
& + I_{1y}I_{2z}\cos\theta\sin\beta. \qquad (7)
\end{aligned}
$$

The solutions shown in Eqs. (4)–(7) provide direct insight into the various terms created for arbitrary flip angles. Using the above expressions Table 1 shows the one-spin order, two-spin order, and zero quantum coherence's (ZQC) created by a 180° flip angle for all the four transitions.

2.2. ABX spin system

When the chemical shift difference between two of the three nuclei (AB) is comparable to their coupling to each other, and both are coupled to a third nucleus (X) with a chemical shift well away from the chemical shifts of other two, the spin system is designated as ABX. Such ABX spectra are common in a number of metabolites, including amino acids present in different tumors. The Hamiltonian for an ABX spin system can be expressed as

$$
\begin{aligned}
H = {} & \omega_1 I_{1z} + \omega_2 I_{2z} + \omega_3 I_{3z} + 2\pi J_{12}(I_{1z}I_{2z} + I_{1x}I_{2x} \\
& + I_{1y}I_{2y}) + 2\pi J_{13}(I_{1z}I_{3z}) + 2\pi J_{23}(I_{2z}I_{3z}), \qquad (8)
\end{aligned}
$$

where I_{1m}, I_{2m}, and I_{3m} are the m-components of the nuclear spin angular momentum operators for A, B, and X nuclei; ω_1, ω_2, and ω_3 are the precession frequencies of the nuclei A, B, and X, respectively. J_{12} indicates the coupling between A and B nuclei, J_{13} is the coupling between A and X nuclei, and J_{23} is the coupling between B and X nuclei. The transition-selective Hamiltonian for the ABX transitions can be defined by employing the eight eigenstates shown in the energy level diagram of Fig. 2. The two sets of AB subspectra are defined by the transitions $|1\rangle\langle 4|$, $|2\rangle\langle 6|$, $|3\rangle\langle 7|$, and $|5\rangle\langle 8|$ and $|1\rangle\langle 3|$, $|2\rangle\langle 5|$, $|4\rangle\langle 7|$, and $|6\rangle\langle 8|$ and the X part of the ABX spectrum is formed by the transitions $|1\rangle\langle 2|$, $|3\rangle\langle 5|$, $|4\rangle\langle 6|$, and $|7\rangle\langle 8|$ and two combination lines $|3\rangle\langle 6|$ and $|4\rangle\langle 5|$. The combination lines usually appear as outerlines in the highfield and lowfield of the X spin multiplet. They are usually referred as three-spin single quantum coherences as it involves absorption of two quanta with simultaneous emission of one quantum [19]. They are more often weak in intensity and disappear in the weakly coupled AMX spectrum. The combination lines are not considered any further in this work. The x phase transition selective pulse Hamiltonian for all transitions of ABX spin system and the solutions for issuing any arbitrary flip angle on these transitions were derived as described for the AB spin system. Considering the symmetry between the sets of AB transitions corresponding to $X = \pm 1/2$ states, it is sufficient to obtain solutions for one set of AB spin transitions. The solution for any arbitrary flip angle for the AB spin transitions $|1\rangle\langle 4|$, $|2\rangle\langle 6|$, $|3\rangle\langle 7|$, and $|5\rangle\langle 8|$ are given by Eqs. (9)–(12).

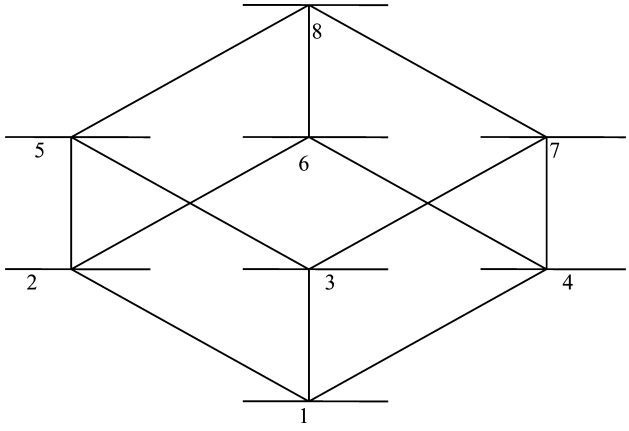

Fig. 2. Energy level diagram of an ABX spin system consisting of three-spin 1/2 nuclei. The numbers correspond to the following eigenstates. 1. $|\alpha\alpha\alpha\rangle$, 2. $|\alpha\alpha\beta\rangle$, 3. $\cos\theta^+|\alpha\beta\alpha\rangle + \sin\theta^+|\beta\alpha\alpha\rangle$, 4. $-\sin\theta^+|\alpha\beta\alpha\rangle + \cos\theta^+|\beta\alpha\alpha\rangle$, 5. $\cos\theta^-|\alpha\beta\beta\rangle + \sin\theta^-|\beta\alpha\beta\rangle$, 6. $-\sin\theta^-|\alpha\beta\beta\rangle + \cos\theta^-|\beta\alpha\beta\rangle$, 7. $|\beta\beta\alpha\rangle$, 8. $|\beta\beta\beta\rangle$ where $\theta^\pm = \frac{1}{2}\tan^{-1}\frac{2\pi J_{AB}}{D^\pm}$ and $D^\pm = \omega_A - \omega_B \pm \pi(J_{AX} - J_{BX})$.

$$
\begin{aligned}
|1\rangle\langle 4| \Rightarrow\ & -\frac{I_{1y}}{4}\cos\theta^+(\sin\beta) + \frac{I_{2y}}{4}\sin\theta^+(\sin\beta) \\
& -\frac{I_{1y}}{2}(I_{2z} + S_z)\cos\theta^+(\sin\beta) + \frac{I_{2y}}{2}(I_{1z} + S_z) \\
& \times \sin\theta^+(\sin\beta) - I_{1y}I_{2z}S_z\cos\theta^+(\sin\beta) \\
& + I_{1z}I_{2y}S_z\sin\theta^+(\sin\beta) \\
& + I_{1z}\left(\frac{1}{4}\cos^2\theta^+(\cos\beta - 1) + 1\right) \\
& + I_{2z}\left(\frac{1}{4}\sin^2\theta^+(\cos\beta - 1) + 1\right) \\
& + \frac{1}{2}I_{1z}I_{2z}(\cos\beta - 1) + \frac{1}{2}I_{1z}S_z\cos^2\theta^+(\cos\beta - 1) \\
& + \frac{1}{2}I_{2z}S_z\sin^2\theta^+(\cos\beta - 1) + I_{1z}I_{2z}S_z(\cos\beta - 1) \\
& + \frac{1}{2}(I_{1x}I_{2x} + I_{1y}I_{2y})\sin\theta^+\cos\theta^+(\cos\beta - 1) \\
& + (I_{1x}I_{2x} + I_{1y}I_{2y})S_z\sin\theta^+\cos\theta^+(\cos\beta - 1), \qquad (9)
\end{aligned}
$$

$$
\begin{aligned}
|2\rangle\langle 6| \Rightarrow\ & -\frac{I_{1y}}{4}\cos\theta^{-}(\sin\beta)+\frac{I_{2y}}{4}\sin\theta^{-}(\sin\beta)\\
& -\frac{I_{1y}}{2}(I_{2z}-S_z)\cos\theta^{-}(\sin\beta)+\frac{I_{2y}}{2}(I_{1z}-S_z)\\
& \times\sin\theta^{-}(\sin\beta)+I_{1y}I_{2z}S_z\cos\theta^{-}(\sin\beta)\\
& -I_{1z}I_{2y}S_z\sin\theta^{-}(\sin\beta)\\
& +I_{1z}\left(\frac{1}{4}\cos^2\theta^{-}(\cos\beta-1)+1\right)\\
& +I_{2z}\left(\frac{1}{4}\sin^2\theta^{-}(\cos\beta-1)+1\right)\\
& -\frac{1}{2}I_{1z}I_{2z}(\cos\beta-1)-\frac{1}{2}I_{1z}S_z\cos^2\theta^{-}(\cos\beta-1)\\
& -\frac{1}{2}I_{2z}S_z\sin^2\theta^{-}(\cos\beta-1)-I_{1z}I_{2z}S_z(\cos\beta-1)\\
& +\frac{1}{2}(I_{1x}I_{2x}+I_{1y}I_{2y})\sin\theta^{-}\cos\theta^{-}(\cos\beta-1)\\
& -(I_{1x}I_{2x}+I_{1y}I_{2y})S_z\sin\theta^{-}\cos\theta^{-}(\cos\beta-1), \qquad (10)
\end{aligned}
$$

$$
\begin{aligned}
|3\rangle\langle 7| \Rightarrow\ & -\frac{I_{1y}}{4}\cos\theta^{+}(\sin\beta)-\frac{I_{2y}}{4}\sin\theta^{+}(\sin\beta)\\
& +\frac{I_{1y}}{2}(I_{2z}-S_z)\cos\theta^{+}(\sin\beta)+\frac{I_{2y}}{2}(I_{1z}-S_z)\\
& \times\sin\theta^{+}(\sin\beta)+I_{1y}I_{2z}S_z\cos\theta^{+}(\sin\beta)\\
& +I_{1z}I_{2y}S_z\sin\theta^{+}(\sin\beta)\\
& +I_{1z}\left(\frac{1}{4}\cos^2\theta^{+}(\cos\beta-1)+1\right)\\
& +I_{2z}\left(\frac{1}{4}\sin^2\theta^{+}(\cos\beta-1)+1\right)\\
& -\frac{1}{2}I_{1z}I_{2z}(\cos\beta-1)+\frac{1}{2}I_{1z}S_z\cos^2\theta^{+}(\cos\beta-1)\\
& +\frac{1}{2}I_{2z}S_z\sin^2\theta^{+}(\cos\beta-1)-I_{1z}I_{2z}S_z(\cos\beta-1)\\
& +\frac{1}{2}(I_{1x}I_{2x}+I_{1y}I_{2y})\sin\theta^{+}\cos\theta^{+}(\cos\beta-1)\\
& +(I_{1x}I_{2x}+I_{1y}I_{2y})S_z\sin\theta^{+}\cos\theta^{+}(\cos\beta-1), \qquad (11)
\end{aligned}
$$

$$
\begin{aligned}
|5\rangle\langle 8| \Rightarrow\ & -\frac{I_{1y}}{4}\cos\theta^{-}(\sin\beta)-\frac{I_{2y}}{4}\sin\theta^{-}(\sin\beta)\\
& +\frac{I_{1y}}{2}(I_{2z}+S_z)\cos\theta^{-}(\sin\beta)+\frac{I_{2y}}{2}(I_{1z}+S_z)\\
& \times\sin\theta^{-}(\sin\beta)-I_{1y}I_{2z}S_z\cos\theta^{-}(\sin\beta)\\
& -I_{1z}I_{2y}S_z\sin\theta^{-}(\sin\beta)\\
& +I_{1z}\left(\frac{1}{4}\cos^2\theta^{-}(\cos\beta-1)+1\right)\\
& +I_{2z}\left(\frac{1}{4}\sin^2\theta^{-}(\cos\beta-1)+1\right)\\
& -\frac{1}{2}I_{1z}I_{2z}(\cos\beta-1)-\frac{1}{2}I_{1z}S_z\cos^2\theta^{-}(\cos\beta-1)\\
& -\frac{1}{2}I_{2z}S_z\sin^2\theta^{-}(\cos\beta-1)+I_{1z}I_{2z}S_z(\cos\beta-1)\\
& +\frac{1}{2}(I_{1x}I_{2x}+I_{1y}I_{2y})\sin\theta^{-}\cos\theta^{-}(\cos\beta-1)\\
& -(I_{1x}I_{2x}+I_{1y}I_{2y})S_z\sin\theta^{-}\cos\theta^{-}(\cos\beta-1). \qquad (12)
\end{aligned}
$$

Using Eqs. (9)–(12) Table 2 shows the one-spin order, two-spin order, and ZQCs created by a 180° flip angle for the AB subspectrum formed by $|1\rangle\langle 4|$, $|2\rangle\langle 6|$, $|3\rangle\langle 7|$, and $|5\rangle\langle 8|$. Similarly the solution for any arbitrary flip angle for the X-spin transitions $|1\rangle\langle 2|$, $|3\rangle\langle 5|$, $|4\rangle\langle 6|$, and $|7\rangle\langle 8|$ are given Eqs. (13)–(16).

$$
\begin{aligned}
|1\rangle\langle 2| \Rightarrow\ & (S_y+2I_{1_z}S_y+2I_{2z}S_y+4I_{1z}I_{2z}S_y)(-\tfrac{1}{4})\\
& \times(\sin\beta)+S_z+(S_z+2I_{1z}S_z+2I_{2z}S_z\\
& +4I_{1z}I_{2z}S_z)(\tfrac{1}{4})(\cos\beta-1), \qquad (13)
\end{aligned}
$$

$$
\begin{aligned}
|3\rangle\langle 5| \Rightarrow\ & -(I_{1z}-I_{2z})\\
& \left(\frac{1}{4}\sin(\theta^{+}+\theta^{-})\sin(\theta^{+}-\theta^{-})(\cos\beta-1)+1\right)\\
& +S_z\left(\frac{\cos\beta-1}{4}+1\right)-I_{1z}I_{2z}S_z t(\cos\beta-1)\\
& +\frac{1}{2}(I_{1z}S_z-I_{2z}S_z)\cos(\theta^{+}+\theta^{-})\\
& \times\cos(\theta^{+}-\theta^{-})(\cos\beta-1)+(I_{1x}I_{2x}+I_{1y}I_{2y})\\
& \times S_z\sin(\theta^{+}+\theta^{-})\cos(\theta^{+}-\theta^{-})\\
& \times(\cos\beta-1)+\frac{1}{2}(I_{1x}I_{2x}+I_{1y}I_{2y})\sin(\theta^{+}-\theta^{-})\\
& \times\cos(\theta^{+}+\theta^{-})(\cos\beta-1)-\frac{S_y}{4}\\
& \times\cos(\theta^{+}-\theta^{-})\sin\beta+(I_{2z}S_y-I_{1z}S_y)\frac{1}{2}\\
& \times\cos(\theta^{+}+\theta^{-})\sin\beta+I_{1z}I_{2z}S_y\cos(\theta^{+}-\theta^{-})\\
& \times\sin\beta-(I_{1x}I_{2x}+I_{1y}I_{2y})S_y\sin(\theta^{+}+\theta^{-})\\
& \times\sin\beta-(I_{1x}I_{2y}-I_{1y}I_{2x})\\
& \times S_x\sin(\theta^{+}-\theta^{-})\sin\beta, \qquad (14)
\end{aligned}
$$

$$
\begin{aligned}
|4\rangle\langle 6| \Rightarrow\ & (I_{1z}-I_{2z})\\
& \times\left(\frac{1}{4}\sin(\theta^{+}+\theta^{-})\sin(\theta^{+}-\theta^{-})(\cos\beta-1)+1\right)\\
& +S_z\left(\frac{\cos\beta-1}{4}+1\right)-I_{1z}I_{2z}S_z(\cos\beta-1)\\
& -\frac{1}{2}(I_{1z}S_z-I_{2z}S_z)(\cos(\theta^{+}+\theta^{-})\\
& \times\cos(\theta^{+}-\theta^{-})(\cos\beta-1))-(I_{1x}I_{2x}+I_{1y}I_{2y})\\
& \times S_z\sin(\theta^{+}+\theta^{-})\cos(\theta^{+}-\theta^{-})\\
& \times(\cos\beta-1)-\frac{1}{2}(I_{1x}I_{2x}+I_{1y}I_{2y})\sin(\theta^{+}-\theta^{-})\\
& \times\cos(\theta^{+}+\theta^{-})(\cos\beta-1)-\frac{S_y}{4}\cos(\theta^{+}-\theta^{-})\\
& \times\sin\beta-(I_{2z}S_y-I_{1z}S_y)\frac{1}{2}\cos(\theta^{+}+\theta^{-})\\
& \times\sin\beta+I_{1z}I_{2z}S_y\cos(\theta^{+}-\theta^{-})\sin\beta\\
& +(I_{1x}I_{2x}+I_{1y}I_{2y})S_y\sin(\theta^{+}+\theta^{-})\sin\beta\\
& -(I_{1x}I_{2y}-I_{1y}I_{2x})S_x\sin(\theta^{+}-\theta^{-})\sin\beta, \qquad (15)
\end{aligned}
$$

Table 2
Longitudinal orders and ZQCs created in the following four AB transitions in ABX spin system by a x phase transition selective pulse with a flip angle $\beta = 180°$

	$\|1\rangle\langle 4\|$	$\|2\rangle\langle 6\|$	$\|3\rangle\langle 7\|$	$\|5\rangle\langle 8\|$
One-spin order	$I_{1z}(-\frac{1}{2}\cos^2\theta^+ + 1)$ $I_{2z}(-\frac{1}{2}\sin^2\theta^+ + 1)$	$I_{1z}(-\frac{1}{2}\cos^2\theta^- + 1)$ $I_{2z}(-\frac{1}{2}\sin^2\theta^- + 1)$	$I_{1z}(-\frac{1}{2}\cos^2\theta^+ + 1)$ $I_{2z}(-\frac{1}{2}\sin^2\theta^+ + 1)$	$I_{1z}(-\frac{1}{2}\cos^2\theta^- + 1)$ $I_{2z}(-\frac{1}{2}\sin^2\theta^- + 1)$
Two-spin order	$-I_{1z}I_{2z}$ $-I_{1z}S_z\cos^2\theta^+$ $-I_{2z}S_z\sin^2\theta^+$	$-I_{1z}I_{2z}$ $I_{1z}S_z\cos^2\theta^-$ $I_{2z}S_z\sin^2\theta^-$	$I_{1z}I_{2z}$ $-I_{1z}S_z\cos^2\theta^+$ $-I_{2z}S_z\sin^2\theta^+$	$I_{1z}I_{2z}$ $I_{1z}S_z\cos^2\theta^-$ $I_{2z}S_z\sin^2\theta^-$
Three-spin order	$-2I_{1z}I_{2z}S_z$	$2I_{1z}I_{2z}S_z$	$2I_{1z}I_{2z}S_z$	$-2I_{1z}I_{2z}S_z$
ZQC	$-(I_{1x}I_{2x} + I_{1y}I_{2y})$ $\sin\theta^+ \times \cos\theta^+$ $-2(I_{1x}I_{2x} + I_{1y}I_{2y})S_z$ $\sin\theta^+ \times \cos\theta^+$	$-(I_{1x}I_{2x} + I_{1y}I_{2y})$ $\sin\theta^- \times \cos\theta^-$ $2(I_{1x}I_{2x} + I_{1y}I_{2y})S_z$ $\sin\theta^- \times \cos\theta^-$	$-(I_{1x}I_{2x} + I_{1y}I_{2y})$ $\sin\theta^+ \times \cos\theta^+$ $-2(I_{1x}I_{2x} + I_{1y}I_{2y})S_z$ $\sin\theta^+ \times \cos\theta^+$	$-(I_{1x}I_{2x} + I_{1y}I_{2y})$ $\sin\theta^- \times \cos\theta^-$ $+2(I_{1x}I_{2x} + I_{1y}I_{2y})S_z$ $\sin\theta^- \times \cos\theta^-$

Table 3
Longitudinal orders and ZQCs created in the following four X spin transitions of ABX spin system by a x phase transition selective pulse with a flip angle $\beta = 180°$

	$\|1\rangle\langle 2\|$	$\|3\rangle\langle 5\|$	$\|4\rangle\langle 6\|$	$\|7\rangle\langle 8\|$
One-spin order	$\frac{S_z}{2}$	$\frac{S_z}{2}$ $-I_{1z} + I_{2z}\begin{bmatrix} -\frac{1}{2}\sin(\theta^+ + \theta^-)\times \\ \sin(\theta^+ - \theta^-) + 1 \end{bmatrix}$	$\frac{S_z}{2}$ $I_{1z} - I_{2z}\begin{bmatrix} -\frac{1}{2}\sin(\theta^+ + \theta^-)\times \\ \sin(\theta^+ - \theta^-) + 1 \end{bmatrix}$	$\frac{S_z}{2}$
Two-spin order	$-I_{1z}S_z$	$-I_{1z}S_z\begin{pmatrix}\cos(\theta^+ + \theta^-)\times \\ \cos(\theta^+ - \theta^-)\end{pmatrix}$	$I_{1z}S_z\begin{pmatrix}\cos(\theta^+ + \theta^-)\times \\ \cos(\theta^+ - \theta^-)\end{pmatrix}$	$I_{1z}S_z$
	$-I_{2z}S_z$	$I_{2z}S_z\begin{pmatrix}\cos(\theta^+ + \theta^-)\times \\ \cos(\theta^+ - \theta^-)\end{pmatrix}$	$-I_{2z}S_z\begin{pmatrix}\cos(\theta^+ + \theta^-)\times \\ \cos(\theta^+ - \theta^-)\end{pmatrix}$	$I_{2z}S_z$
Three-spin order	$-2I_{1z}I_{2z}S_z$	$2I_{1z}I_{2z}S_z$	$2I_{1z}I_{2z}S_z$	$-2I_{1z}I_{2z}S_z$
ZQC		$-(I_{1x}I_{2x} + I_{1y}I_{2y})$ $\sin(\theta^+ - \theta^-) \times \cos(\theta^+ + \theta^-)$ $-2(I_{1x}\ I_{2x} + I_{1y}I_{2y})S_z$ $\sin(\theta^+ + \theta^-) \times \cos(\theta^+ - \theta^-)$	$(I_{1x}I_{2x} + I_{1y}I_{2y})$ $\sin(\theta^+ - \theta^-) \times \cos(\theta^+ + \theta^-)$ $2(I_{1x}\ I_{2x} + I_{1y}I_{2y})S_z$ $\sin(\theta^+ + \theta^-) \times \cos(\theta^+ - \theta^-)$	

$$
\begin{aligned}
|7\rangle\langle 8| \Rightarrow (&-S_y + 2I_{1_z}S_y + 2I_{2z}S_y \\
&- 4I_{1z}I_{2z}S_y)\left(\frac{1}{4}\right)(\sin\beta) + S_z \\
&+ (-S_z + 2I_{1z}S_z + 2I_{2z}S_z \\
&- 4I_{1z}I_{2z}S_z)\left(-\frac{1}{4}\right)(\cos\beta - 1). \qquad (16)
\end{aligned}
$$

Table 3 shows the results obtained from Eqs. (13)–(16) for 180° flip angle on the X spin transitions.

3. Experimental

3.1. Experimental data

All experiments were performed on a Varian Unity 600 MHz high resolution NMR system. The frequency cycling experiment [12] was programmed using the Varian software (VNMR). This approach involves frequency-selective inversion of a single transition, followed by a hard pulse of fixed phase and optimum flip angle, phase alternating the receiver on successive scans when the selective inversion frequency is incremented. This approach requires at least one well resolved multiplet in the spectrum. Longitudinal multispin orders have to be reconverted to observable magnetization with a flip angle less than 90°. The optimum reconversion pulse flip angle ϕ for longitudinal order is given by the $\phi = \sin^{-1}[\frac{1}{\sqrt{N}}]$ where N refers to the size of the order [12]. Using this expression the optimum flip angle ϕ for reconversion of two-spin order is 45° and for three-spin order amounts to 35°. Selective excitation was achieved using low power, long duration Gaussian shaped pulses. The lengths of these pulses were tailored to achieve sufficient selectivity in the frequency domain without perturbing the nearest line depending on the magnitude of the J coupling. The duration of the pulses applied varied from 200 to 300 ms. Trisodium citrate dissolved in D_2O was used as an AB spin system. Styrene dibromide dissolved in CDCl3 includes a ABX spin system.

3.2. Simulated data

To verify the solutions for the transition selective pulses on AB and ABX spin systems to separate the various longitudinal orders theoretical simulations was

performed using NMR-SCOPE program [17]. The one pulse experiment was simulated by single hard pulse followed by detection period under strong coupling evolution. The frequency cycling experiment was simulated by transition selective Gaussian pulse followed by a optimum θ° hard pulse. On successive scans the selective inversion frequency was incremented. The strong coupling evolution was employed during the detection period. The receiver phase was determined from the theoretical solutions shown for $\beta = 180^\circ$ in Table 1 for AB and Tables 2 and 3 for ABX spin system.

4. Results and discussion

Fig. 3 shows the results from experiments performed on trisodium citrate (AB spin system). Fig. 3A shows the spectrum obtained with a single pulse. The J coupling between the two protons involved is 15 Hz and the chemical shift separation between them is 80 Hz clearly indicating a AB spin system. Fig. 3B shows the two-spin order spectrum obtained from the same molecule using the frequency cycling approach. The solutions shown in Table 1 for $\beta = 180^\circ$ clearly indicate that when a frequency cycle of $(+1, -2)$ or $(-1, +2)$ is run on $|1\rangle\langle 2|$, $|3\rangle\langle 4|$ or $|1\rangle\langle 3|$, $|2\rangle\langle 4|$ transitions pure two-spin order can be separated from all other one-spin order and ZQCs, regardless of the coupling strength. The two-spin order spectrum shown was created with a frequency cycle of $(+1, -2)$ on transitions $|1\rangle\langle 2|$, $|3\rangle\langle 4|$. The prefixed sign on the frequency cycle indicates the receiver acquisition phase. The simulated spectra of trisodium citrate is shown in Fig. 4. Fig. 4A shows the one pulse simulation and Fig. 4B shows two-spin order simulation obtained by running the same frequency cycle employed for experimental spectrum. Note the excellent agreement between the experimental and theoretical spectra.

Table 2 shows the various terms created in the AB subspectra ($|1\rangle\langle 4|$, $|2\rangle\langle 6|$, $|3\rangle\langle 7|$, and $|5\rangle\langle 8|$) by a 180° pulse. The results indicate that the frequency cycling experiment can be performed in one of the two AB subspectra to separate the AB two-spin order from all other longitudinal orders and ZQCs by running a frequency cycle of -1, -2, $+3$, $+4$ or $+1$, $+2$, -3, -4 from low field transition to high field transition. Fig. 5 shows the experimental spectra from styrene dibromide. Fig. 5A shows the ABX part of the spectrum obtained by a single pulse. The chemical shift separation between A and B spins is 30 Hz and the J_{AB} is -11 Hz. The chemical shift separation between A and X nuclei is 673 Hz and between B and X is 643 Hz. The J_{BX} coupling is 10.5 Hz and J_{AX} coupling is 5 Hz. Fig. 5B shows the AB two-spin order spectrum obtained by running a frequency cycle of -1, -2 $+3$, $+4$ on the low field AB multiplet where all the four transitions are resolved. Table 2 also indicates that we can separate ABX three-spin order by running a frequency cycle of -1, $+2$, $+3$, -4 or

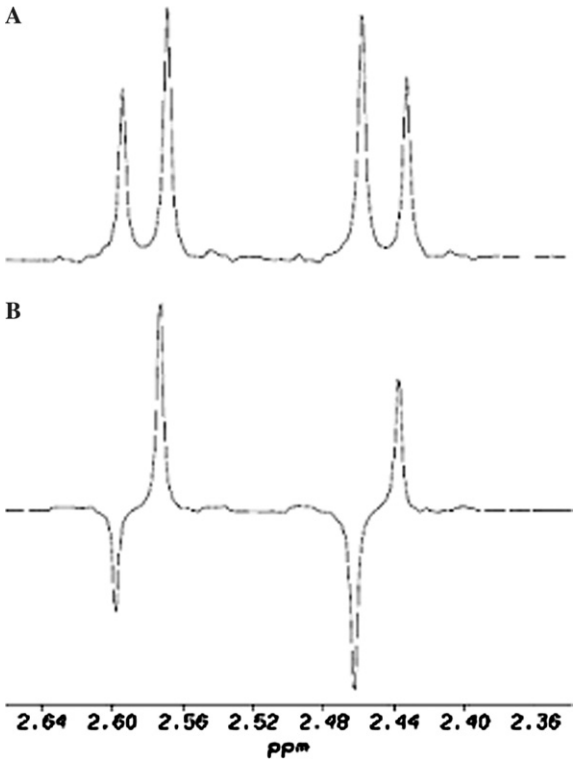

Fig. 3. Experimental spectra of trisodium citrate. (A) One pulse spectrum of trisodium citrate obtained with single scan. (B) Two-spin order spectrum of trisodium citrate obtained with two scans by running a frequency cycle of 1, -2 on the low field doublet.

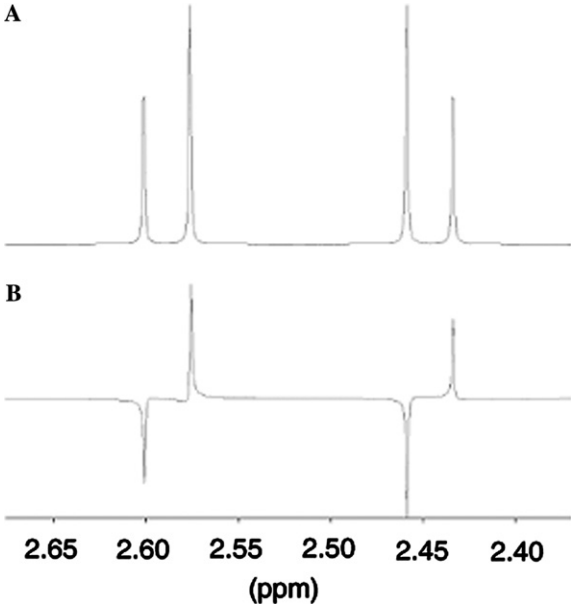

Fig. 4. Simulated spectra of trisodium citrate. (A) One pulse simulation. (B) Two-spin order simulation obtained by running a frequency cycle of 1, -2 on the low field doublet.

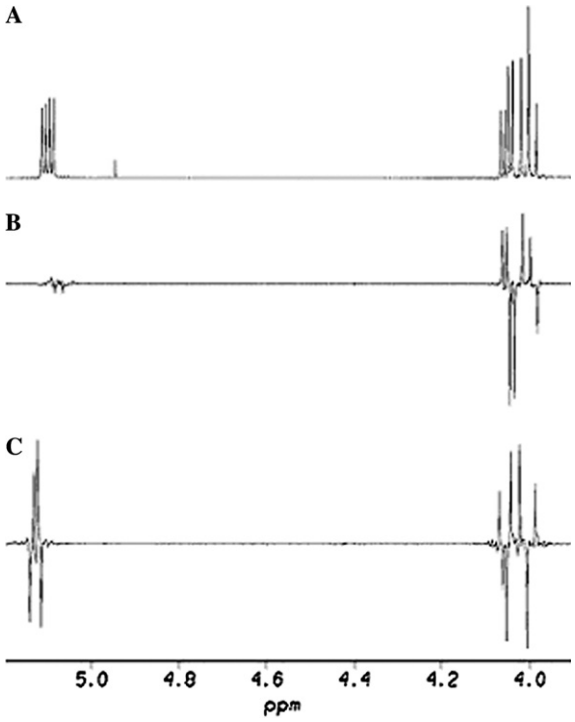

Fig. 5. Experimental spectra of styrene dibromide. (A) ABX part of the spectrum obtained by a single pulse. (B) Two-spin order (AB) spectrum obtained with four scans by running a frequency cycle of −1, −2, +3, +4 on the low field AB multiplet. (C) Three-spin order spectrum obtained with four scans by running a frequency cycle of −1, +2, +3, −4 on the X spin transitions.

+1, −2, −3, +4 on one of the AB multiplets. Table 3 shows the various terms created in the four X spin transitions by a 180° pulse. It is possible to separate the ABX three-spin order by running a frequency cycle of −1, +2, +3, −4 or +1,−2, −3, +4 on the X spin transitions $|1\rangle\langle 2|$, $|3\rangle\langle 5|$, $|4\rangle\langle 6|$, and $|7\rangle\langle 8|$. Fig. 5C shows the ABX three-spin order spectrum obtained by running a frequency cycle of −1, +2, +3, −4 on the X spin transitions. Fig. 6 shows the simulated spectra of styrene dibromide. Fig. 6A shows the one pulse simulation and Fig. 6B shows the AB two-spin order simulation obtained with same frequency cycle as employed for the experimental spectrum shown in Fig. 5B. Note the simulated AB two-spin order spectrum resolves the overlapping transition in the high field AB multiplet which is not seen in the experimental spectrum due to the cancellation of the antiphase signal by line broadening. Fig. 6C shows the three-spin order simulation obtained by the same frequency cycle employed for experimental spectrum shown in Fig. 5C. From Tables 2 and 3 it is clear that we cannot separate the AX or BX two-spin order independent of the strong coupling parameter. The results indicate that this approach can be employed for separating and analyzing the longitudinal orders in broad range of spin systems that exhibit strong coupling.

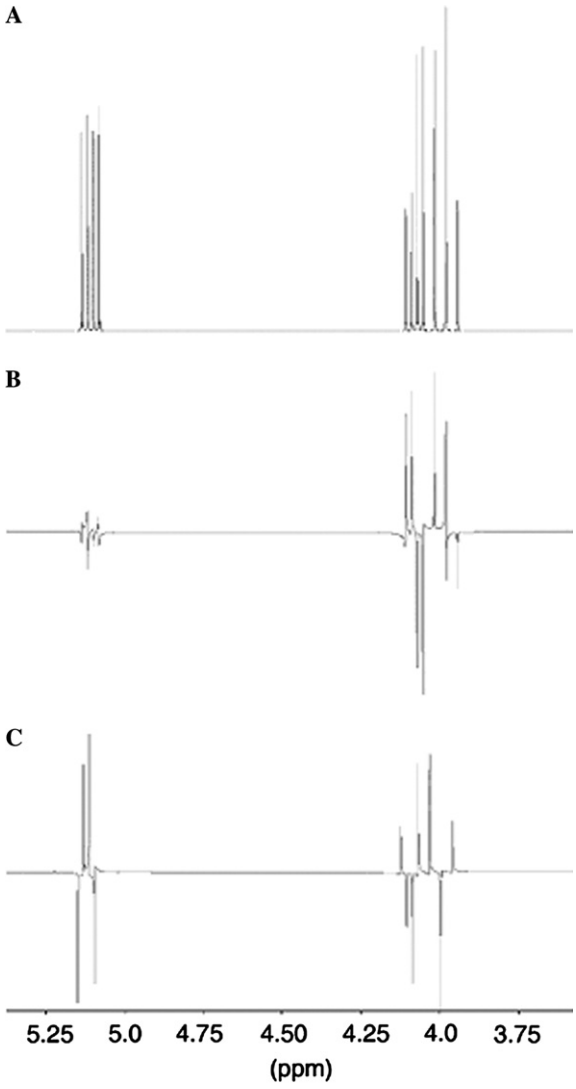

Fig. 6. Simulated spectra of styrene dibromide. (A) One pulse simulation. (B) Two-spin order simulated spectrum by frequency cycle of −1, −2, +3, +4 on the low field AB multiplet. (C) Three-spin order simulated spectrum obtained by frequency cycle of −1, +2, +3, −4 on the X multiplet.

5. Conclusions

Longitudinal orders have been investigated in strongly coupled AB and ABX spin systems. Solutions are given for any arbitrary flip angle for all transitions in both these spin systems. Experimental and theoretical spectra of longitudinal orders are shown for these spin systems. This work might lead to applications in metabonomics for studying in vivo metabolic profiles; spectral editing techniques at clinical field strengths using longitudinal orders and also to improve quantification of metabolites when detected through longitudinal order pathways. Other applications include determination of relative sign of scalar couplings and measurement of relaxation rates of longitudinal multispin orders.

Acknowledgments

This research was supported by a WVU Health Science Center Internal Grant. I thank Prof. N. Chandrakumar, IIT, Madras for the scientific discussions; Dr. R.R. Raylman, Radiology, WVU for advice on experimental design; Dr. Igor Goljer from Varian, Inc. for help on programming issues; and Prof. Demilly Graveron, Laboratoire de RMN, CNRS, France for providing the NMR-SCOPE program.

References

[1] R.R. Ernst, G. Bodenhausen, A. Wokaun, Principles of Nuclear Magnetic Resonance in One and Two Dimensions, Clarendon Press, Oxford, 1987.
[2] M.H. Levitt, Spin Dynamics, Wiley, England, 2001.
[3] D. Canet, Construction, evolution and detection of magnetization modes designed for treating longitudinal relaxation of weakly coupled spin 1/2 systems with magnetic equivalence, Prog. NMR Spectrosc. 21 (1989) 237–291.
[4] L.D. Bari, J. Kowalewski, G. Bodenhausen, Magnetization transfer modes in scalar-coupled spin systems investigated by selective two-dimensional nuclear magnetic resonance exchange experiments, J. Chem. Phys. 93 (1990) 7698–7705.
[5] G. Ziegler, H. Sterk, W. Bermal, Relaxation of an AX_2 nuclear spin system. Amplitude modulated pulses for excitation of longitudinal multispin ordered states, J. Chem. Phys. 101 (1994) 7248–7254.
[6] O.W. Sørensen, R.R. Ernst, Design of pulse sequences sensitive to relative signs of J coupling constants. Corrections to the SLAP experiment, J. Magn. Reson. 63 (1985) 219–224.
[7] G. Bodenhausen, G. Wagner, M. Rance, O.W. Sørensen, K. Wuthrich, R.R. Ernst, Longitudinal two-spin order in 2D exchange spectroscopy, J. Magn. Reson. 59 (1984) 542–550.
[8] P. Mutzenhardt, D. Canet, Behavior of longitudinal spin orders in NMR measurements of self-diffusion coefficients using radiofrequency field gradients, J. Chem. Phys. 105 (1996) 4405–4411.
[9] I.M. Brereton, S.E. Rose, G.J. Galloway, L.N. Moxon, D.M. Doddrell, In vivo volume selective metabolite editing via correlated z-order, J. Magn. Reson. 16 (1990) 460–469.
[10] R.R. Reddy, V.H. Subramanian, B.J. Clark, J.S. Leigh, Longitudinal spin-order-based pulse sequence for lactate editing, Magn. Reson. Med. 19 (1991) 477–482.
[11] R.A. deGraaf, D.L. Rothman, Detection of γ-aminobutyric acid (GABA) by longitudinal scalar order difference editing, J. Magn. Reson. 152 (2001) 124–131.
[12] N. Chandrakumar, S. Sendhil Velan, Separation of longitudinal multispin order by frequency cycling, J. Magn. Reson. A 104 (1993) 363–365.
[13] D.M. Doddrell, D.T. Pegg, M.R. Bendall, Distortionless enhancement of NMR signals by polarization transfer, J. Magn. Reson. 48 (1982) 323–327.
[14] J.A. Pople, W.G. Schneider, H.J. Bernstein, High Resolution Nuclear Magnetic Resonance, McGraw-Hill, USA, 1959.
[15] J.W. Emsley, J. Feeney, L.H. SutcliffeHigh Resolution Nuclear Magnetic Resonance Spectroscopy, vol. 1, Pergamon Press, London, 1965.
[16] L.E. Kay, R.E.D. McClung, A product operator description of AB and ABX spin systems, J. Magn. Reson. 77 (1988) 258–273.
[17] D. Graveron-Demilly, A. Diop, A. Briguet, B. Fenet, Product operator algebra for strongly coupled spin systems, J. Magn. Reson. A 101 (1993) 233–239.
[18] L.C. Costello, R.B. Franklin, P. Narayan, Citrate in the diagnosis of prostate cancer, Prostate 38 (1999) 237–245.
[19] R. Freeman, Spin Choreography, Oxford University Press, New York, 1997.